Deformations and dynamics of an elastic string in a periodic potential

Peter Ziswiler
Theoretische Physik, ETH-Hönggerberg, CH-8093 Zürich, Switzerland

Vadim Geshkenbein
Theoretische Physik, ETH-Hönggerberg, CH-8093 Zürich, Switzerland
and L.D. Landau Institute for Theoretical Physics, 117940 Moscow, Russia

Gianni Blatter
Theoretische Physik, ETH-Hönggerberg, CH-8093 Zürich, Switzerland
(Received 19 February 1997)

We study the dissipative dynamics of a driven elastic string subject to a periodic potential. The deformations of the elastic string are determined in the static and dynamic situations for various geometries. We find the average velocity of the string, particularly the dependence of the velocity on the mean angle ϑ between the string and the potential. Our theoretical analysis produces both a sharp drop in the average velocity at small angles due to the trapping of the elastic string in the potential and a crossover from free motion to a pinning-inhibited motion at the critical driving force. [S0163-1829(97)05525-2]

I. INTRODUCTION

Recent interest has concentrated on dynamical aspects of driven elastic manifolds subject to a pinning potential. Both periodic[1] and random[2,3] potentials have been studied in various contexts. Typical questions addressed are the relation between the average velocity and the underlying driving force,[3] the critical behavior at depinning,[2] the dynamical reestablishing of order,[4–6] etc. In this paper we present a model study of one of the simplest problems in this context, namely, the dissipative motion of a driven elastic string subject to a periodic (washboard) potential. Besides its educational character, this problem is relevant for the understanding of vortices in layered high-T_c superconductors. The problem has been addressed before by Büttiker and Landauer,[1] who calculated the energy for kink-antikink production and determined the activated dynamics through the solution of the Fokker-Planck equation. Recently, Koshelev and Vinokur[7] have determined the corrections to the Ohmic resistivity at large driving force, making use of the dynamical approach.[8,9]

Here, we consider the flow of an elastic string in a periodic (washboard) potential subject to a constant transverse driving force **F**. The mean angle ϑ between the string and the potential is fixed through the boundary conditions; see Fig. 1. The basic task consists in solving the partial differential equation describing the balance between the driving force and forces due to the elasticity, the friction, and the potential. To investigate small forces, we determine the deformations of the string in the static situation for various geometries and use these results to compute the dynamics. At large forces, we make use of the dynamical approach in order to study the strongly driven string. A numerical analysis finally solves the problem in the intermediate regime.

Our analysis yields both a sharp drop in the velocity at small angles pointing to the trapping of the elastic string in the potential wells and the velocity-force characteristic over the entire range of applied driving forces, where the linear regimes at small and large driving forces are connected through a nonlinear crossover at forces close to the depinning force F_c; see Fig. 2.

In Sec. II, we present our model of the elastic string in the periodic (washboard) potential. The static solution to this model is determined in Sec. III. In Sec. IV we introduce the partial differential equation describing the driven string. This equation is solved analytically for small and large driving forces F in comparison with the critical force F_c due to the potential. A numerical evaluation finally determines the deformations of the elastic string and the average velocity for all driving forces F.

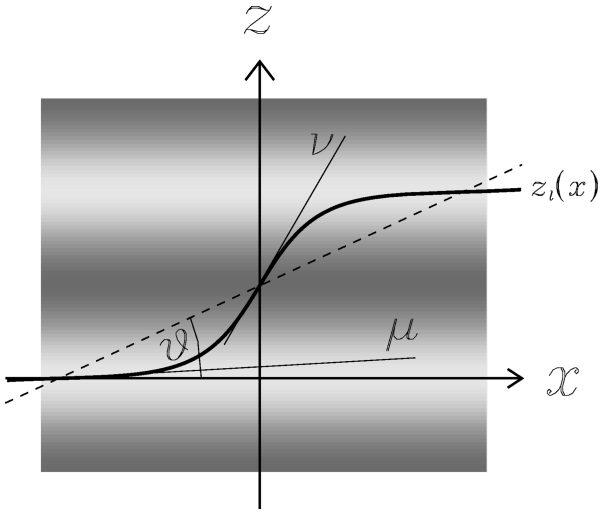

FIG. 1. Elastic string $z_l(x)$ in the pinning potential $V(z)=v_l[1-\cos(2\pi z/d)]$. The x axis lies in a potential valley, whereas the z axis threads the potential hills perpendicularly . The mean angle ϑ between the string and the x axes is fixed through periodic boundary conditions. μ and ν denote the *slope* of the string in the valleys and on the hills, respectively.

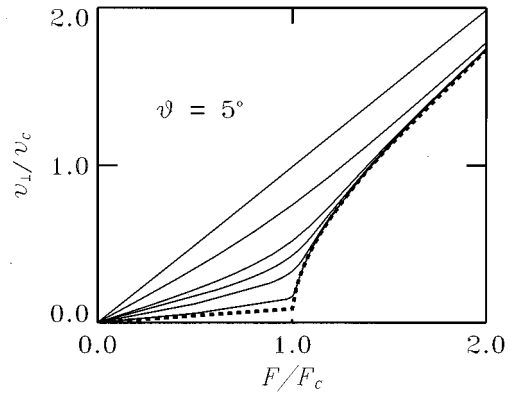

FIG. 2. Average transverse string velocity $v_\perp$ vs applied driving force F. The different lines correspond to increasing potential strength $v_l/\varepsilon_l=0.001$, 0.01, 0.03, 0.05, 0.1, and 1 at an angle $\vartheta=5°$. The dashed line indicates the limit $v_l\to\infty$.

II. MODEL

We consider a string with elasticity ε_l in a potential of the form $V(z)=v_l[1-\cos(2\pi z/d)]$ with d the period and v_l the strength of the potential. We choose a coordinate system where the string comes to lie in the xz plane with a shape given by the function $z_l(x)$. The mean angle ϑ of the string with respect to the potential is fixed through the boundary conditions; see Fig. 1. The string is driven by a transverse force **F** (**F** is locally orthogonal to the string and has the constant magnitude F) and its motion is impeded by the friction force $\mathbf{F}_\eta=-\eta_l\hat{\mathbf{v}}$, where η_l is the friction coefficient and $\hat{\mathbf{v}}$ denotes the local velocity orthogonal to the string. Our model describes an idealized vortex line with constant line tension ε_l in a layered superconductor. The potential $V(z)$ then corresponds to the intrinsic pinning potential due to the layered structure with d denoting the distance between layers. The constant transverse force **F** corresponds to the Lorentz force $\mathbf{F}_L=(\Phi_0/c)\mathbf{j}\wedge\mathbf{n}$, where **n** is the unit vector along the vortex, $\Phi_0=hc/2e\approx 2\times10^{-7}$ G cm^2 is the flux quantum, and **j** denotes an external applied current density. The friction coefficient η_l is given by the Bardeen-Stephen expression[10] $\eta_l=\Phi^2/2\pi c^2\rho_n\xi^2$, with ρ_n the normal-state resistivity of the material and ξ the coherence length. The mean angle ϑ between the vortex line and the layers is fixed in a nontrivial way through the external magnetic field **H**; see Ref. 11.

The investigation of driven vortex lines in layered superconductors is supposed to explain a number of interesting phenomena. In order to establish dissipation-free current flow, the vortex lines have to be pinned such that $\mathbf{v}=0$ in spite of $\mathbf{F}_L\neq0$. Therefore, the possibility of intrinsic pinning and the trapping of vortices in the potential wells has recently attracted a great deal of attention.[7,12] Experimentally, these features can be investigated by performing resistive measurements at small misalignments of magnetic field with respect to the layers. Precise angular measurements of the linear resistivity have been carried out by Kwok *et al.*[13] for $YBa_2Cu_3O_{7-\delta}$ (YBCO) single crystals and by Iye *et al.*[14] for thin films of $Bi_2Sr_2Ca_7Cu_2O_8$ (BiSCCO).

III. STATIC SOLUTION

In a first attack we consider a string $z_l(x)$ with elasticity ε_l in the potential $V(z)=v_l[1-\cos(2\pi z/d)]$. The mean angle ϑ with respect to the potential is determined through the boundary condition $z_l(x+\Delta x)=z_l(x)+d$ with $\Delta x=d/\tan\vartheta$. The shape of the string is determined by the competition between its elasticity and the energy gain in the potential. We then have to minimize the energy functional

$$\mathcal{F}[z_l]=\int dx\sqrt{1+z_l'^2}\left\{\varepsilon_l+v_l\left[1-\cos\left(\frac{2\pi z_l}{d}\right)\right]\right\}, \quad (1)$$

where $\sqrt{1+z_l'^2}dx$ gives the length of a line element $d\mathbf{s}$ and the prime denotes the derivative with respect to x. Variation of this functional with respect to the function $z_l(x)$ furnishes the equation determining the shape of the string,

$$-\frac{z_l''}{(1+z_l'^2)^{3/2}}\left\{\varepsilon_l+v_l\left[1-\cos\left(\frac{2\pi z_l}{d}\right)\right]\right\}+\frac{1}{(1+z_l'^2)^{1/2}}v_l\frac{2\pi}{d}\sin\left(\frac{2\pi z_l}{d}\right)=0. \quad (2)$$

Multiplying Eq. (2) by z_l' and integrating yields

$$\frac{d}{dx}\left(\frac{1}{\sqrt{1+z_l'^2}}\left\{\varepsilon_l+v_l\left[1-\cos\left(\frac{2\pi z_l}{d}\right)\right]\right\}\right)=0, \quad (3)$$

and integrating Eq. (3) once more [we make use of the boundary conditions $z_l(0)=d/2$ and $\partial z_l/\partial x|_{x=0}\equiv\nu$] produces the relation

$$\sqrt{1+z_l'^2}=\frac{\sqrt{1+\nu^2}}{1+2v_l/\varepsilon_l}\left[1+\frac{2v_l}{\varepsilon_l}\sin^2\left(\frac{\pi z_l}{d}\right)\right]. \quad (4)$$

The slope μ of the string in a potential valley is then determined through the equation

$$1+\mu^2=\frac{1+\nu^2}{(1+2v_l/\varepsilon_l)^2}. \quad (5)$$

Since μ has to be larger than zero, the range of ν is restricted through the condition

$$\nu\geq 2\sqrt{\frac{v_l}{\varepsilon_l}}\sqrt{1+\frac{v_l}{\varepsilon_l}}, \quad (6)$$

where the limit $\mu=0$, $1+\nu^2=(1+2v_l/\varepsilon_l)^2$ describes a string with only one kink, in the following referred to $\vartheta=0^+$.

The integration of Eq. (4) determines the shape of the string in the potential through

$$x(z_l)=\int_{d/2}^{z_l}dz\left[(1+\nu^2)\left(\frac{1+2(v_l/\varepsilon_l)\sin^2(\pi z/d)}{1+2(v_l/\varepsilon_l)}\right)^2-1\right]^{-1/2}. \quad (7)$$

The relation between the slope ν and the mean angle ϑ of the string with respect to the potential is determined through the boundary condition

$$\tan\vartheta=\frac{-d}{x(-d/2)}. \quad (8)$$

In the *small-angle limit* $\vartheta=0^+$ we find the following results:

$$x(z_l)=\frac{d}{2\pi}\sqrt{\frac{\varepsilon_l}{v_l}}\int_{\pi/2}^{\pi z_l/d}\frac{dt}{\sin t\sqrt{1+(v_l/\varepsilon_l)\sin^2 t}}$$

$$\cong\begin{cases}\dfrac{d}{2\pi}\sqrt{\dfrac{\varepsilon_l}{v_l}}\ln\left[\tan\left(\dfrac{\pi z_l}{2d}\right)\right], & \dfrac{v_l}{\varepsilon_l}\ll 1,\\ -\dfrac{d}{2\pi}\dfrac{\varepsilon_l}{v_l}\cot\left(\dfrac{\pi z_l}{d}\right), & \dfrac{v_l}{\varepsilon_l}\gg 1,\end{cases}\tag{9}$$

or, after inversion, the line shape $z_l(x)$ reads

$$z_l(x)\cong\begin{cases}\dfrac{2d}{\pi}\arctan\left(\exp\left[2\pi\sqrt{\dfrac{v_l}{\varepsilon_l}}\dfrac{x}{d}\right]\right), & \dfrac{v_l}{\varepsilon_l}\ll 1,\\ \dfrac{d}{\pi}\operatorname{arccot}\left(-2\pi\dfrac{v_l}{\varepsilon_l}\dfrac{x}{d}\right), & \dfrac{v_l}{\varepsilon_l}\gg 1.\end{cases}\tag{10}$$

Equation (10) gives the horizontal extension of the kink through the length scale

$$L_k\approx\begin{cases}d\sqrt{\dfrac{\varepsilon_l}{v_l}}, & \dfrac{v_l}{\varepsilon_l}\ll 1,\\ d\dfrac{\varepsilon_l}{v_l}, & \dfrac{v_l}{\varepsilon_l}\gg 1.\end{cases}\tag{11}$$

In addition we obtain the kink energy

$$\mathcal{E}_{\rm kink}=\int_{-\infty}^{\infty}\left[\left(\varepsilon_l+2v_l\sin^2\frac{\pi z_l}{d}\right)\sqrt{1+z_l'^2}-\varepsilon_l\right]dx,\tag{12}$$

where $z_l(x)$ denotes the shape of the string in the limit $\vartheta=0^+$. The integration in Eq. (12) can most easily be performed with the help of Eq. (4) in the limit $1+\nu^2=(1+2v_l/\varepsilon_l)^2$ and by carrying out the substitution $\tilde{z}=\pi z_l(x)/d, d\tilde{z}=[\pi z_l'(x)/d]dx$ with $z_l(-\infty)=0$ and $z_l(\infty)=d$. With a few algebraic manipulations we arrive at

$$\mathcal{E}_{\rm kink}=\frac{2d}{\pi}\left[\sqrt{v_l\varepsilon_l}+(\varepsilon_l+v_l)\arcsin\frac{1}{\sqrt{1+\varepsilon_l/v_l}}\right]$$

$$\cong\begin{cases}\dfrac{4d}{\pi}\sqrt{v_l\varepsilon_l}\left[1-\dfrac{v_l}{3\varepsilon_l}+O\left(\dfrac{v_l^2}{\varepsilon_l^2}\right)\right], & \dfrac{v_l}{\varepsilon_l}\ll 1,\\ dv_l\left[1+\dfrac{\varepsilon_l}{v_l}+O\left(\dfrac{\varepsilon_l^{3/2}}{v_l^{3/2}}\right)\right], & \dfrac{v_l}{\varepsilon_l}\gg 1.\end{cases}\tag{13}$$

The results (11) and (13) for small ratios $v_l/\varepsilon_l\ll 1$ can also be obtained from a dimensional comparison of the tilt energy with the potential energy,

$$\mathcal{E}_{\rm tilt}\approx\varepsilon_l\frac{d^2}{L_k}\approx v_l L_k\approx\mathcal{E}_{\rm pot}\Rightarrow L_k\approx d\sqrt{\frac{\varepsilon_l}{v_l}},$$

$$\mathcal{E}_{\rm kink}\approx d\sqrt{v_l\varepsilon_l}.\tag{14}$$

Second, we investigate the *large-angle domain* $\vartheta\lesssim\pi/2$. Here, we can expand Eq. (7) for large ν and find

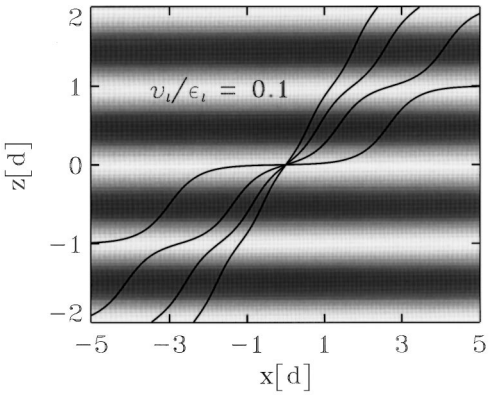

FIG. 3. Static string configurations at different angles $\vartheta=10°,20°,30°$, and $40°$ for $v_l/\varepsilon_l=0.1$.

$$x(z_l)\cong\frac{1+2v_l/\varepsilon_l}{\nu}\int_{d/2}^{z_l}\frac{dz}{1+(2v_l/\varepsilon_l)\sin^2(\pi z/d)}$$

$$=\frac{d\sqrt{1+2v_l/\varepsilon_l}}{\pi\nu}\left\{\arctan\left[\sqrt{1+2v_l/\varepsilon_l}\tan\left(\frac{\pi z_l}{d}\right)\right]-\frac{\pi}{2}\right\}.\tag{15}$$

Using the boundary condition $x(0)=-d/2\tan\vartheta$ and inverting, we determine the line shape as

$$z_l(x)\cong\frac{d}{\pi}\arctan\left[\frac{1}{\sqrt{1+2v_l/\varepsilon_l}}\tan\left(\frac{\pi\tan\vartheta}{d}x+\frac{\pi}{2}\right)\right]$$

$$(\tan\vartheta\gg 1,-d/\tan\vartheta<x<0).\tag{16}$$

In the limit $v_l/\varepsilon_l\ll 1$, Eq. (16) reduces to a straight line $z_l(x)=x\tan\vartheta+d/2$. An estimate for the crossover angle ϑ_k, separating the domain where the string is kinked from that where it remains straight, can most simply be obtained from Eq. (11):

$$\vartheta_k\approx\begin{cases}\arctan\left(\dfrac{d}{L_k}\right)=\arctan\left(\sqrt{\dfrac{v_l}{\varepsilon_l}}\right), & \dfrac{v_l}{\varepsilon_l}\ll 1,\\ \arctan\left(\dfrac{v_l}{\varepsilon_l}\right), & \dfrac{v_l}{\varepsilon_l}\gg 1.\end{cases}\tag{17}$$

A few line shapes at different angles ϑ are shown in Fig. 3.

IV. DRIVEN SOLUTION

Consider the motion of an elastic string in the potential $V(z)$ resulting from the transverse driving force **F** and the counteracting friction force $\mathbf{F}_\eta=-\eta_l\hat{\mathbf{v}}$. Our goal is to determine the mobility α defined through the equation

$$v_\perp=\alpha F,\tag{18}$$

where $v_\perp$ is the average transverse string velocity.

To derive a differential equation for this situation, we let the string move with constant velocity v in the x direction, assuming its shape to be preserved during motion, i.e., $z_l(x,t)\equiv z_l(x-vt)$. The equation of motion is found by balancing the driving force against the sum of friction, elastic, and potential forces acting on the line element $d\mathbf{s}$,

$$F=\eta_l(\mathbf{v}\cdot\mathbf{n}_\perp)-\frac{\delta\mathcal{F}}{\delta z_l}. \tag{19}$$

Here,

$$\mathbf{n}_\perp=\frac{1}{\sqrt{1+z_l'^2}}\begin{pmatrix} z_l' \\ -1\end{pmatrix}$$

is a vector of unit length perpendicular to the line element $d\mathbf{s}$ in the direction of $\mathbf{F}$, $\mathbf{v}=(v,0)$, and the variational derivative of the functional (1) gives the forces orthogonal to the line due to the elasticity and the potential. Multiplying Eq. (19) by z_l', we obtain an equation analogous to Eq. (3), which additionally accounts for the driving and friction forces,

$$\frac{d}{dx}\left(\frac{1}{\sqrt{1+z_l'^2}}\left\{\varepsilon_l+v_l\left[1-\cos\left(\frac{2\pi z_l}{d}\right)\right]\right\}\right)$$

$$=\eta_l v\frac{z_l'^2}{\sqrt{1+z_l'^2}}-Fz_l'. \tag{20}$$

In the following, we first derive some analytical results for the differential equation (20) in the limit of small and large driving forces F and then solve it numerically in a second step.

A. Linear response to $F\ll(2\pi/d)v_l$

Let us first consider a small driving force F. We then follow an approach introduced by Gor'kov and Kopnin[15,16] (see also Dorsey[17]) to obtain a solvability condition. The solution $z_l(x)$ will be close to the static solution $z_0(x)$ with the velocity v being the small parameter in our analysis. We consider perturbations from the static solution by expanding the function $z_l(x)$ in powers of the velocity v, $z_l(x)=z_0(x)+z_1(x)$. $z_0(x)$ then solves the equilibrium equation (3) and $z_1(x)$ gives the correction of order v due to the driving force, with the $O(v)$ equation taking the form

$$\frac{d}{dx}\left(-\frac{z_0'}{(1+z_0'^2)^{3/2}}\left\{\varepsilon_l+v_l\left[1-\cos\left(\frac{2\pi z_0}{d}\right)\right]\right\}z_1'\right.$$

$$\left.+\frac{v_l(2\pi/d)\sin(2\pi z_0/d)}{(1+z_0'^2)^{1/2}}z_1\right)=\eta_l v\frac{z_0'^2}{(1+z_0'^2)^{1/2}}-Fz_0'. \tag{21}$$

In the next step, we integrate Eq. (21) over a period Δx of the string. In doing so, we impose the boundary condition $z_1'(-\Delta x/2)=z_1'(\Delta x/2)$ and make use of the periodic boundary conditions for $z_0(x)$. The left-hand side of Eq. (21) becomes zero, leaving only the integral over the friction and driving forces,

$$0=\int_{-\Delta x/2}^{\Delta x/2}dx\left\{\eta_l v\frac{z_0'^2}{(1+z_0'^2)^{1/2}}-Fz_0'\right\}. \tag{22}$$

Performing the integration of the second term with the help of the boundary values for $z_0(x)$, we finally obtain the steady-state velocity

$$v=\frac{F}{\eta_l}\left(\frac{1}{d}\int_{-\Delta x/2}^{\Delta x/2}dx\,\frac{z_0'^2}{(1+z_0'^2)^{1/2}}\right)^{-1}. \tag{23}$$

Note that only the static solution contributes to the velocity v; i.e., the parameters F and η_l do not appear in the shape $z_0(x)$ of the line. Equation (23) is our solvability condition for steady motion and is exact to linear order in the velocity v. If we directly integrate Eq. (20) over a period of the string, we obtain the same expression for the velocity v except that we have to replace the static solution $z_0(x)$ by the unknown driven solution $z_l(x)$. Alternatively, the solvability condition can be obtained from a comparison between the dissipated power and the power fed into the string through the driving force F, i.e.,

$$\int_{-\Delta x/2}^{\Delta x/2}d\mathbf{s}\,[\eta_l(\mathbf{v}\cdot\mathbf{n}_\perp)](\mathbf{v}\cdot\mathbf{n}_\perp)=\int_{-\Delta x/2}^{\Delta x/2}d\mathbf{s}F(\mathbf{v}\cdot\mathbf{n}_\perp). \tag{24}$$

The driving force F does not depend on the shape of the string. On the contrary the friction force depends on the local velocity and is large for segments orthogonal to the potential but small in the opposite case. The different behavior of the friction and driving forces will give rise to a large-angle anomaly to be discussed in Sec. IV B below.

In the following we are mainly interested in the response $\alpha=v_\perp/F\equiv v\sin\vartheta/F$ normal to the string. For a small potential $v_l/\varepsilon_l\ll1$ and for large angles ϑ the string is almost straight providing us with the approximation

$$z_0(x)\approx x\tan\vartheta\ \Rightarrow\ \alpha\cong\alpha_0\equiv\frac{1}{\eta_l}; \tag{25}$$

i.e., the motion is not disturbed by the potential $V(z)$. The other extreme is realized for the large-potential or for the small-angle limit, where only the kinks with steep slopes z_0' contribute to the integral. In this case we obtain

$$\int_{-\Delta x/2}^{\Delta x/2}dx\,\frac{z_0'^2}{\sqrt{1+z_0'^2}}\cong\int_{\text{kink}}dxz_0'=d$$

$$\Rightarrow\ v\cong\frac{F}{\eta_l},\quad \alpha\cong\alpha_0\sin\vartheta$$

$$\left(\vartheta<\arctan\frac{v_l}{\varepsilon_l},\quad \frac{v_l}{\varepsilon_l}\gg1\right), \tag{26}$$

where the angular domain is restricted by the condition (17) derived in the static situation. For the general case we express z_0' in terms of z_0 by using Eq. (4). With the substitution $\tilde{z}=\pi z_0(x)/d$, $d\tilde{z}=[\pi z_0'(x)/d]dx$, we arrive at the result

$$\alpha=\alpha_0\frac{\sin\vartheta}{J(v_l/\varepsilon_l,\nu)},$$

$$J\left(\frac{v_l}{\varepsilon_l},\nu\right)=\frac{2}{\pi}\int_0^{\pi/2}d\tilde{z}\,\sqrt{1-\frac{1}{1+\nu^2}\left(\frac{1+2v_l/\varepsilon_l}{1+2(v_l/\varepsilon_l)\sin^2\tilde{z}}\right)^2}, \tag{27}$$

where ν is related to ϑ via Eq. (8). In Fig. 4 we show the renormalization factor $J(v_l/\varepsilon_l,\nu)$ as a function of the angle ϑ. We recognize two characteristic domains, one at large

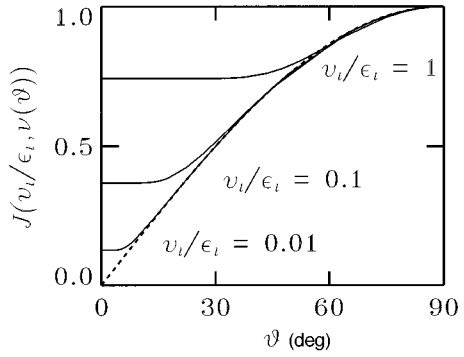

FIG. 4. $J(v_l/\varepsilon_l,\nu(\vartheta))$ as a function of the angle ϑ. J is roughly equal to $\sin\vartheta$ at large angles and becomes constant at small angles. The dashed line indicates $\sin\vartheta$.

angles where J is roughly equal to $\sin\vartheta$ and another domain at small angles where $J(v_l/\varepsilon_l,\nu)\equiv J_0(v_l/\varepsilon_l)$ is constant, most easily determined in the limit $\vartheta=0^+$,

$$J_0\left(\frac{v_l}{\varepsilon_l}\right)=\frac{4\sqrt{v_l/\varepsilon_l}}{\pi}\int_0^{\pi/2}d\tilde{z}\,\frac{\sin\tilde{z}}{1+2(v_l/\varepsilon_l)\sin^2\tilde{z}}\sqrt{1+\frac{v_l}{\varepsilon_l}\sin^2\tilde{z}}; \tag{28}$$

see Fig. 5. The mobility α is thus given through the approximations

$$\frac{\alpha}{\alpha_0}\approx\begin{cases}\dfrac{\sin\vartheta}{J_0(v_l/\varepsilon_l)}, & \vartheta<\vartheta_t\equiv\arcsin J_0(v_l/\varepsilon_l),\\ 1, & \vartheta>\vartheta_t,\end{cases}$$

$$\approx\begin{cases}\dfrac{\pi}{4\sqrt{v_l/\varepsilon_l}}\left[1+\dfrac{v_l}{\varepsilon_l}\right]\sin\vartheta, & 0<\dfrac{v_l}{\varepsilon_l}\ll 1,\quad \vartheta<\vartheta_t,\\ \left[1+\dfrac{0.2399}{\sqrt{v_l/\varepsilon_l}}\right]\sin\vartheta, & \dfrac{v_l}{\varepsilon_l}\gg 1,\quad \vartheta<\vartheta_t,\end{cases} \tag{29}$$

where we introduced the trapping angle ϑ_t separating the two angular domains. For $\vartheta<\vartheta_t$ the string is trapped in the potential valleys and α decreases as ϑ for $\vartheta\to 0$, whereas for $\vartheta>\vartheta_t$ the potential does not affect the motion. In comparison with the earlier discussion of Eq. (23) we conclude that for $\vartheta\lesssim\vartheta_t$ the motion is well described by the motion of kinks and $1/J_0$ gives only a correction factor of order unity to this finding. In the limit of small ratios $v_l/\varepsilon_l\ll 1$, the trapping angle ϑ_t is of the same order as the crossover angle ϑ_k. In the limit of large ratios $v_l/\varepsilon_l\gg 1$, however, the trapping happens at angles smaller than the crossover angle ϑ_k. An expansion for the corresponding limits yields the following dependences:

$$\vartheta_t\sim\sqrt{\frac{v_l}{\varepsilon_l}}\sim\vartheta_k,\quad \frac{v_l}{\varepsilon_l}\ll 1,$$

$$\vartheta_t\cong\frac{\pi}{2}-0.69\left(\frac{\varepsilon_l}{v_l}\right)^{1/4},\quad \vartheta_k\cong\frac{\pi}{2}-\frac{\varepsilon_l}{v_l},\quad \frac{v_l}{\varepsilon_l}\gg 1. \tag{30}$$

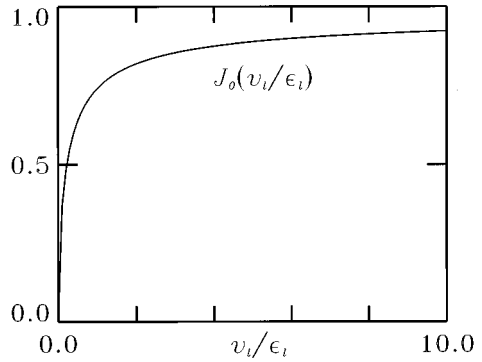

FIG. 5. J_0 as a function of the ratio v_l/ε_l. For $v_l/\varepsilon_l>1$, J_0 is of order unity.

Figure 6 shows the scaled mobility α/α_0. We observe a sharp drop in the mobility for small angles ϑ, particularly for small ratios $v_l/\varepsilon_l\ll 1$. This drop is well described by the renormalization factor $J_0(v_l/\varepsilon_l)/\sin\vartheta$ as already pointed out above. Figure 6 shows further an unexpected effect of our model at large angles ϑ. We observe a string moving faster in the presence of the potential than in the undisturbed case, leading to a mobility $\alpha>\alpha_0$. We postpone a discussion of this large-angle anomaly to the following subsection.

B. Dynamic approach, $F\gg(2\pi/d)v_l$

We proceed with a study of large driving forces F, where the potential leads to merely small perturbations away from the free motion. While the static solution determined the shape in the linear response, the string is now well described by a straight line. Accordingly, we start from the free motion and consider the potential as a small perturbation in our analysis. An adequate way is to follow a dynamical approach similar to the one used by Koshelev and Vinokur.[7] In a first step, we rotate the coordinate system of Eq. (19) such that the string is parallel to the new $\tilde{x}$ axis; see Fig. 7. Second, we allow for an arbitrary time-dependent string shape $\tilde{z}_l(\tilde{x},t)$. The friction force F_η is given by

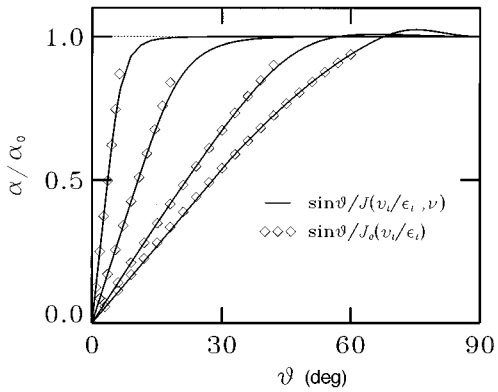

FIG. 6. The mobility α as a function of the angle ϑ for the ratios $v_l/\varepsilon_l=0.01$, 0.1, 1, and 10. The drop in the mobility becomes sharper for decreasing ratios v_l/ε_l and is well described by $\sin\vartheta/J_0(v_l/\varepsilon_l)$ at small angles $\vartheta<\vartheta_t$. The large-angle anomaly ($\alpha>\alpha_0$) is investigated within the dynamic approach.

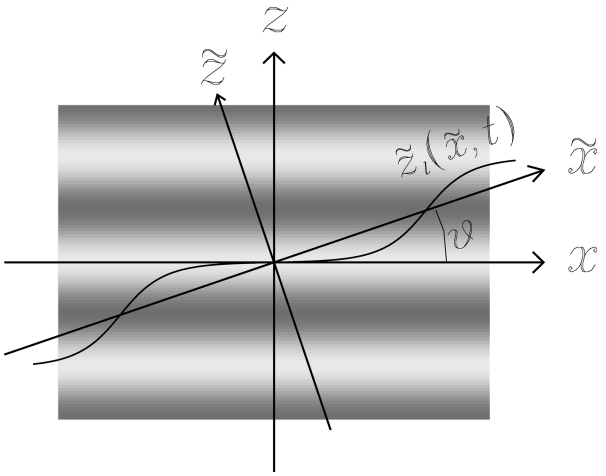

FIG. 7. Coordinate system used in the dynamic approach. The $\tilde{x}$ axis is aligned with the string.

$$F_\eta = -\frac{\eta_l}{\sqrt{1+\tilde{z}_l'^2}}\frac{\partial \tilde{z}_l(\tilde{x},t)}{\partial t}. \tag{31}$$

The free energy $\mathcal{F}$ takes the form

$$\mathcal{F} = \int d\tilde{x}\sqrt{1+\tilde{z}_l'^2}\{\varepsilon_l + v_l\,[1-\cos(\mathbf{n}_z\cdot\mathbf{r})]\}, \tag{32}$$

where $\mathbf{n}_z$ is the unit vector along the z direction in the new coordinate system,

$$\mathbf{n}_z = \begin{pmatrix}\sin\vartheta\\ \cos\vartheta\end{pmatrix} \quad \text{and} \quad \mathbf{r} = \frac{2\pi}{d}\begin{pmatrix}\tilde{x}\\ \tilde{z}_l\end{pmatrix}.$$

Upon rotation and making use of the friction force (31) and the free energy (32), the differential equation (19) takes the form

$$\begin{aligned}\varepsilon_l\tilde{z}_l'' - \eta_l\dot{\tilde{z}}_l(1+\tilde{z}'^2) = v_l\Big[&-\tilde{z}_l''[1-\cos(\mathbf{n}_z\cdot\mathbf{r})] + \frac{2\pi}{d}(\cos\vartheta\\ &-\tilde{z}_l'\sin\vartheta)(1+\tilde{z}_l'^2)\sin(\mathbf{n}_z\cdot\mathbf{r})\Big]\\ &+F(1+\tilde{z}_l'^2)^{3/2},\end{aligned} \tag{33}$$

where the primes and the overdots denote derivatives with respect to $\tilde{x}$ and t, respectively. Using the ansatz $\tilde{z}_l(\tilde{x},t) = -v_\perp t + u(\tilde{x},t)$ with $v_\perp \equiv F/\eta_l$ and expanding up to order F_c/F [it turns out that $u, u', u'' \sim O(F_c/F)$ and $\dot{u}\sim O(1)$, $F_c \equiv 2\pi v_l/d$ denoting the critical force associated with the potential], we obtain

$$\begin{aligned}\varepsilon_l u'' - \eta_l\dot{u} = v_l\Big[&-u''[1-\cos(\mathbf{n}_z\cdot\mathbf{r})] + u\left(\frac{2\pi}{d}\cos\vartheta\right)^2\\ &\times\cos(\mathbf{n}_z\cdot\mathbf{r}) + \frac{2\pi}{d}(\cos\vartheta - u'\sin\vartheta)\sin(\mathbf{n}_z\cdot\mathbf{r})\Big]\\ &+\frac{1}{2}Fu'^2,\\ \mathbf{n}_z\cdot\mathbf{r} = \frac{2\pi}{d}&(\tilde{x}\sin\vartheta - v_\perp t\cos\vartheta).\end{aligned} \tag{34}$$

In the following, we denote the right-hand side of Eq. (34) by $F_{\rm pin}(u(\tilde{x},t),\tilde{x},t)$. In order to solve Eq. (34), we introduce the elastic Greens function

$$G(\tilde{x},t) = \int\frac{d\omega}{2\pi}\int\frac{dk}{2\pi}\frac{e^{i(k\tilde{x}-\omega t)}}{i\omega\eta_l - k^2\varepsilon_l} = \frac{e^{(-\eta_l/4\varepsilon_l t)\tilde{x}^2}}{\sqrt{4\pi\varepsilon_l\eta_l t}} \tag{35}$$

for the free problem

$$\varepsilon_l\frac{\partial^2 G}{\partial\tilde{x}^2} - \eta_l\frac{\partial G}{\partial t} = \delta(\tilde{x})\,\delta(t).$$

The deformation $u(\tilde{x},t)$ is then given by

$$u(\tilde{x},t) = \int dx\,ds\,G(\tilde{x}-x,t-s)F_{\rm pin}(u(x,s),x,s). \tag{36}$$

To first order in the potential, we insert $u\equiv 0$ in $F_{\rm pin}(u(x,s),x,s)$ and determine the small corrections $u^{(1)}(\tilde{x},t)$ to the shape of the string,

$$u^{(1)}(\tilde{x},t) = C\left[\frac{F}{F_c}\cos(\mathbf{n}_z\cdot\mathbf{r}) + \frac{\varepsilon_l}{v_l}\sin\vartheta\tan\vartheta\sin(\mathbf{n}_z\cdot\mathbf{r})\right],$$

$$\mathbf{n}_z\cdot\mathbf{r} = \frac{2\pi}{d}(\tilde{x}\sin\vartheta - v_\perp t\cos\vartheta),$$

$$C = -\frac{d}{2\pi}\left[\left(\frac{F}{F_c}\right)^2 + \left(\frac{\varepsilon_l}{v_l}\sin\vartheta\tan\vartheta\right)^2\right]^{-1}. \tag{37}$$

The motion is given by the trivial time dependence $\tilde{z}_l(\tilde{x},t) = -v_\perp t + u(\tilde{x},t)$ describing a string moving with the constant velocity $v = v_\perp/\sin\vartheta$ in the x direction. The time dependence of $u(\tilde{x},t)$ is thus periodic with the period T determined by

$$Tv\cos\vartheta = \frac{d}{\sin\vartheta} \;\Rightarrow\; T = \frac{d}{v_\perp\cos\vartheta}.$$

Corrections $\delta v_\perp$ to the velocity $v_\perp = F/\eta_l$ are generated by the force $F_{\rm pin}(u(\tilde{x},t),\tilde{x},t)$ acting on the string. Since we are interested in the mean velocity $v_\perp$, we have to calculate the average value of the pinning force $F_{\rm pin}$,

$$\langle F_{\rm pin}(u(\tilde{x},t),\tilde{x},t)\rangle \equiv \frac{\sin\vartheta}{d}\int_0^{d/\sin\vartheta} F_{\rm pin}(u(\tilde{x},t),\tilde{x},t)\,d\tilde{x}.$$

Note that the periodic time dependence of $F_{\rm pin}$ drops out by this averaging. The correction $\delta v_\perp$ to the velocity $v_\perp$ is given by

$$\eta_l\delta v_\perp = \langle F_{\rm pin}(u^{(1)}(\tilde{x},t),\tilde{x},t)\rangle.$$

Performing the averaging, we finally arrive at

$$\frac{\delta v_\perp}{v_\perp} = \frac{\sin^2\vartheta - 2\cos^2\vartheta}{4}\left[\left(\frac{F}{F_c}\right)^2 + \left(\frac{\varepsilon_l}{v_l}\sin\vartheta\tan\vartheta\right)^2\right]^{-1}. \tag{38}$$

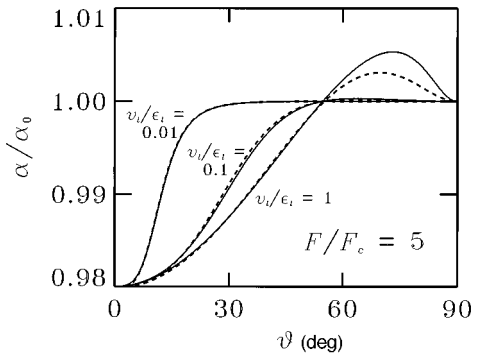

FIG. 8. The mobility α/α_0 as a function of the angle ϑ. Scaling the driving force F with the critical force $F_c=2\pi v_l/d$ renders the mobility at $\vartheta=0°$ independent of v_l. The dashed lines indicate the numerical results. For large ratios v_l/ε_l, the dynamic approach overestimates the large-angle anomaly.

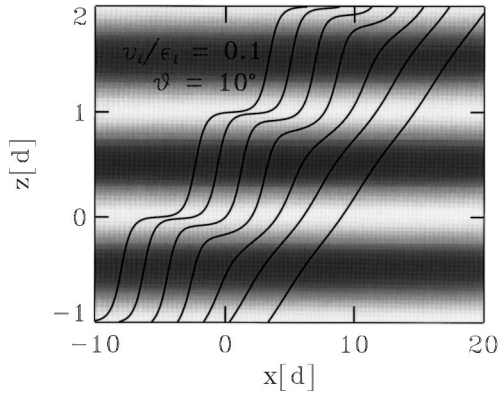

FIG. 9. Deformations of a string with increasing driving force $F/F_c=0.01$, 0.1, 0.5, 1, 2, 5, and 10. For $F\leqslant F_c$ the string keeps its shape while being pushed against the potential walls. At $F\gg F_c$ the string rapidly becomes straight.

With

$$\frac{\delta v_\perp}{v_\perp}\propto v_l^2\cos^2\vartheta\,|G(k=2\pi\sin\vartheta/d,\omega=v_\perp k\cot\vartheta)|^2,$$

the correction $\delta v_\perp$ is mainly determined through the competition between the pinning potential and the intrinsic properties of the string as expressed through its Greens function. The prefactor $\sin^2\vartheta-2\cos^2\vartheta$ consists of a negative term due to the potential force in the $\tilde{z}$ direction $[\propto v_l\cos^2\vartheta\cos(\mathbf{n}_z\cdot\mathbf{r})]$ and a positive term arising from the nonlinear contribution $\frac{1}{2}F\langle u'^2\rangle$. The potential force in the $\tilde{x}$ direction $[\propto v_l\sin\vartheta\sin(\mathbf{n}_z\cdot\mathbf{r})]$ cancels with the force arising from the curvature of the string in the presence of the potential $(\propto v_l[1-\cos(\mathbf{n}_z\cdot\mathbf{r})])$. We further recognize that the friction coefficient η_l does not appear in Eq. (38). The correction $\delta v_\perp$ is only important for $\vartheta\approx 0$ and becomes negligible for increasing angles ϑ. This feature is particularly pronounced for small ratios $v_l/\varepsilon_l\ll 1$; see Fig. 8.

Investigating Eq. (38), we find a positive correction $\delta v_\perp$ for

$$\sin^2\vartheta>2\cos^2\vartheta\;\Rightarrow\;\vartheta>\arctan\sqrt{2}=54.7°,$$

confirming the large-angle anomaly found in linear response (small v). The positive correction to $v_\perp$ occurs due to the fact that the nonlinearities in the friction and the driving force do not cancel each other with the nonlinear (in u) term $\frac{1}{2}F\langle u'^2\rangle$ remaining in the pinning force.

Alternatively, Eq. (38) is obtained by transforming the solvability condition (23) into our new coordinate system, i.e.,

$$\frac{\alpha}{\alpha_0}=d\sin\vartheta\left(\int_{-d/2\sin\vartheta}^{d/2\sin\vartheta}\frac{(\sin\vartheta+\tilde{z}'\cos\vartheta)^2}{\sqrt{1+\tilde{z}'^2}}d\tilde{x}\right)^{-1}$$
$$\approx 1-\frac{2\cos^2\vartheta-\sin^2\vartheta}{2d\sin\vartheta}\int_{-d/2\sin\vartheta}^{d/2\sin\vartheta}\tilde{z}'^2 d\tilde{x},\quad \tilde{z}'\ll 1, \tag{39}$$

and by inserting $u^{(1)}(\tilde{x},t)$ for $\tilde{z}(\tilde{x})$. Equation (39) shows that a slightly bent string $(\tilde{z}'\neq 0)$ moves faster than a straight one at angles $\vartheta>54.7°$. Since the angular dependence of the mobility is determined through the dissipated power (the power fed into the string through the driving force is independent on the string shape), the large-angle anomaly occurs due to the fact that a class of bent strings dissipates less energy than straight ones. In the Appendix we estimate the magnitude of this anomaly with a simple variational ansatz. We find that the anomaly can occur at angles $\vartheta\gtrsim 38.2°$ and can reach its largest value at an angle $\vartheta\approx 68.5°$ where $\alpha/\alpha_0\lesssim 1.055$.

C. Numerical analysis

We have solved the differential equation (19) numerically by a shooting method as described in Ref. 18. We are then able to investigate the deformations of the string in the dynamic situation and to find the dependence of the velocity over the full range of applied driving forces F for different ratios v_l/ε_l. We measure the driving force F in units of the critical force $F_c=2\pi v_l/d$. The velocity $v_\perp$ is measured in units of the velocity v_c describing the motion of a string driven by F_c at an angle $\vartheta=90°$, and thus $v_c=F_c/\eta_l$; summarizing,

$$\frac{F}{F_c}=\frac{dF}{2\pi v_l}\quad\text{and}\quad\frac{v_\perp}{v_c}=\frac{\eta_l v\sin\vartheta}{F}\frac{F}{F_c}=\frac{\alpha}{\alpha_0}\frac{F}{F_c}. \tag{40}$$

The deformations of the string with increasing driving forces F are shown in Fig. 9. We observe a smooth crossover from the static solution derived in Sec. III to a straight line for applied forces $F\gg F_c$. As long as the driving force F is smaller than F_c, the string approximatly keeps its shape as given through the static solution. The only effect of the applied force F is to push the string segments parallel to the x axis against the potential wells. In the linear response of Sec. IVA we pointed out that the solvability condition (23) is rendered exact by replacing the static through the driven solution. Since $z_l(x)$ does not much differ from the static solution $z_0(x)$ as long as $F\leqslant F_c$, we expect a good accuracy of our linear response findings up to driving forces matching the potential forces.

Figures 2 and 10 show the dependence of the average velocity $v_\perp$ on the applied driving force F for different

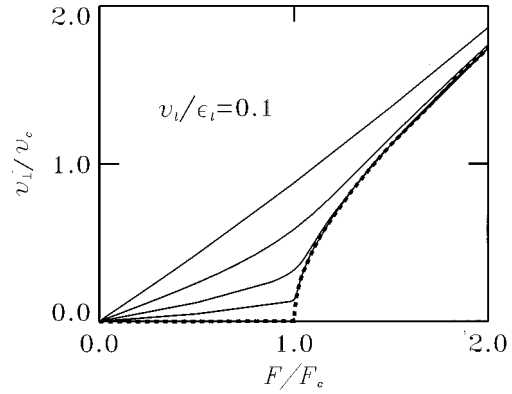

FIG. 10. Force-velocity characteristic at different angles $\vartheta=2°$, 5°, 10°, and 20° for the ratio $v_l/\varepsilon_l=0.1$. The dashed line indicates the limit $\vartheta=0°$.

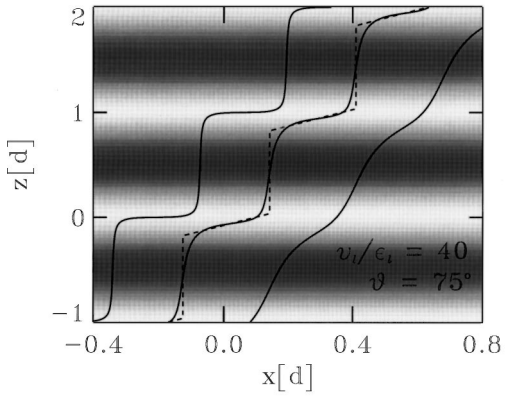

FIG. 11. Comparison of driven strings ($F/F_c=0.002$, 0.6, and 5) with our variational result (dashed line) for $\mu=\tan\vartheta_1$ and $\nu\to\infty$. The string leading to the largest anomly has a shape roughly given through our variational result. Note that we shifted $z_{\mu\nu}(x)$ in the z direction due to the finite driving force.

angles ϑ and for different potential strength v_l/ε_l. We observe two Ohmic regimes for forces F smaller and much larger than the critical force F_c. The mobility at small forces $F\leqslant F_c$ is well determined through Eq. (27) of our linear response, as we have already noted in the discussion of the previous figure. At $F=F_c$ the string is able to move over the potential barriers leading to a rapidly growing velocity and hence to a larger mobility. In the limit of $F\gg F_c$ the potential has almost no effect on the mobility and we find the simple expression $\alpha=F/\eta_l$. For both increasing angles ϑ and decreasing ratios v_l/ε_l, we establish a crossover from the kinked solution (large perturbation due to the potential) to the undisturbed solution, where the force-velocity characteristic is Ohmic for all applied forces F.

In the limit $\vartheta=0°$, the string is trapped for $F<F_c$. Larger forces give rise to a steady motion determined through the equation

$$\eta_l\frac{\partial z_l}{\partial t}=-F-v_l\frac{2\pi}{d}\sin\left(\frac{2\pi z_l}{d}\right). \tag{41}$$

Note that $z_l(x,t)$ is a constant function of x, and therefore Eq. (41) describes the motion of a particle with zero mass and friction coefficient η_l in the potential $Fz+v_l[1-\cos(2\pi z/d)]$. Integrating Eq. (41), we arrive at

$$t(z)=-\frac{1}{v_c}\int_0^{z_l}\frac{dz}{F/F_c+\sin(2\pi z/d)}, \tag{42}$$

where we imposed the boundary condition $z_l(t=0)=0$. The time for moving over one period of the potential is then given by

$$T=t(-d/2)-t(d/2)=\frac{d}{v_c\sqrt{(F/F_c)^2-1}}. \tag{43}$$

The mean velocity $v_\perp$ in units of v_c is finally determined by

$$\frac{v_\perp}{v_c}=\frac{d}{Tv_c}=\sqrt{(F/F_c)^2-1},\quad \vartheta=0°,\quad F\geqslant F_c. \tag{44}$$

This result was also obtained by Aslamazov and Larkin[19] in their study of superconducting point contacts. If we expand Eq. (44) to first order in F_c/F, $F\gg F_c$, we find again the result of the dynamic approach at $\vartheta=0°$. The limit $v_l/\varepsilon_l\to\infty$ at finite angles ϑ is more difficult to investigate. As long as $F\leqslant F_c$ the string has the shape of a staircase leading to a purely kink motion, i.e., $\alpha/\alpha_0=\sin\vartheta$. For $F\geqslant F_c$ we interpolate between the result of the dynamic approach and Eq. (44) to obtain

$$\frac{v_\perp}{v_c}=\sqrt{(F/F_c)^2-\cos^2\vartheta},\quad v_l/\varepsilon_l\to\infty,\quad F\geqslant F_c, \tag{45}$$

in good agreement with our numerical results.

V. CONCLUSION

We have presented a model of a driven, elastic string in a periodic potential and have determined both the force-velocity characteristic and the angular dependence of the mobility over the entire range of applied driving forces. In the limit of small potentials $v_l\ll\varepsilon_l$, the string motion is affected only within the small-angle regime $\vartheta<\sqrt{v_l/\varepsilon_l}$, where a sharp drop in the mobility is observed. Large potentials $v_l\gg\varepsilon_l$ deform the string to produce a staircase shape leading to a kink motion described by the mobility $\alpha=\alpha_0\sin\vartheta$. Increasing the driving force leads to a crossover from the pinning-inhibited motion to the free motion at the depinning force F_c. An unexpected effect appears in the large-angle limit, where the string can move faster than in the free situation.

A comparison of our findings with the experimental data of driven vortex lines in layered superconductors shows a qualitative agreement with the findings of Kwok *et al.*[13] and Iye *et al.*,[14] who observed a trapping of the vortex lines between the layers. Their results, however, exhibit a smoother behavior around vortex trapping. Including thermal fluctuations, the interaction between neighboring vortices, and the internal structure of a vortex line (giving rise to an angle-dependent friction coefficient and line tension) should lead to the desired improvements of our results. The appearence of the large-angle anomaly in the vortex mobility (velocity overshooting) has to be checked in further experiments.

ACKNOWLEDGMENT

It is a pleasure to thank Rolf Heeb for his assistance in all sorts of computational problems.

APPENDIX: MAGNITUDE OF THE ANOMALY

We determine the magnitude of the anomaly with a simple variational ansatz $z_{\mu\nu}(x)$ for the solvability condition (23), where $z_{\mu\nu}(x)$ describes a string consisting of straight pieces with μ,ν denoting the slope in the valleys and on the hills, respectively (see the dashed line in Fig. 11).

Evaluating the integral in the solvability condition (23), we arrive at

$$I(\mu,\nu)\equiv\int_{-d/2\tan\vartheta}^{d/2\tan\vartheta}\frac{z'^{\,2}_{\mu\nu}}{\sqrt{1+z'^{\,2}_{\mu\nu}}}dx$$

$$=\frac{d}{\tan\vartheta}\left[\frac{\mu^2}{\sqrt{1+\mu^2}}\frac{\nu-\tan\vartheta}{\nu-\mu}+\frac{\nu^2}{1+\nu^2}\frac{\tan\vartheta-\mu}{\nu-\mu}\right]$$

$$(\mu\leqslant\tan\vartheta\leqslant\nu). \tag{A1}$$

In the regime $\vartheta\geqslant\vartheta_1\equiv\arctan(\sqrt{\sqrt{5}-1}/\sqrt{2})\approx 38.2°$, the integral $I(\mu,\nu)$ has its absolute minimum in the limit $\nu\to\infty$, $\mu=\sqrt{\sqrt{5}-1}/\sqrt{2}$ independent of ϑ, whereas at smaller angles the straight line yields the smallest value.[20] At the angle $\vartheta=\vartheta_2\equiv\arctan(\sqrt{\sqrt{5}+1}\sqrt{2})\approx 68.5°$, the mobility reaches its largest value given through $\alpha/\alpha_0\approx 1.055$. The mobility determined for a string at an angle ϑ is thus restricted through the extremal values

$$\frac{\alpha}{\alpha_0}(\vartheta)\Big|_{\max}=\begin{cases}1, & \vartheta\leqslant\vartheta_1,\\ \dfrac{\sin\vartheta}{1-\dfrac{1}{\tan\vartheta}\sqrt{\dfrac{5\sqrt{5}-11}{2}}}, & \vartheta\geqslant\vartheta_1,\\ 1.055, & \vartheta=\vartheta_2.\end{cases} \tag{A2}$$

In Fig. 11 we compare our variational result with a string producing a large anomaly.

[1] M. Büttiker and R. Landauer, Phys. Rev. A **23**, 1397 (1981).
[2] O. Narayan and D. S. Fisher, Phys. Rev. B **48**, 7030 (1993).
[3] M. Dong, M. C. Marchetti, A. A. Middleton, and V. Vinokur, Phys. Rev. Lett. **70**, 662 (1993).
[4] A. E. Koshelev and V. M. Vinokur, Phys. Rev. Lett. **73**, 3580 (1994).
[5] L. Balents and M. P. A. Fisher, Phys. Rev. Lett. **75**, 4270 (1995).
[6] T. Giamarchi and P. Le Doussal, Phys. Rev. Lett. **76**, 3408 (1996).
[7] A. E. Koshelev and V. M. Vinokur, Phys. Rev. B **51**, 11 678 (1995).
[8] A. Schmid and W. Hauger, J. Low Temp. Phys. **11**, 667 (1973).
[9] A. I. Larkin and Yu. N. Ovchinnikov, Zh. Eksp. Teor. Fiz. **65**, 1704 (1973) [Sov. Phys. JETP **38**, 854 (1974)].
[10] J. Bardeen and M. J. Stephen, Phys. Rev. A **140**, 1197 (1965).
[11] A. V. Balatskii, L. I. Burlachkov, and L. P. Gor'kov, Zh. Eksp. Teor. Fiz. **90**, 1478 (1986) [Sov. Phys. JETP **63**, 866 (1986)].
[12] D. Feinberg and C. Villard, Phys. Rev. Lett. **65**, 919 (1990).
[13] W. K. Kwok, U. Welp, V. M. Vinokur, S. Fleshler, J. Downey, and G. W. Crabtree, Phys. Rev. Lett. **67**, 390 (1991).
[14] Y. Iye, T. Tamegai, and S. Nakamura, Physica C **174**, 227 (1991).
[15] L. P. Gor'kov and N. B. Kopnin, Zh. Eksp. Teor. Fiz. **60**, 2331 (1971) [Sov. Phys. JETP **33**, 1251 (1971)].
[16] L. P. Gor'kov and N. B. Kopnin, Usp. Fiz. Nauk **116**, 413 (1975) [Sov. Phys. Usp. **18**, 496 (1975)].
[17] A. T. Dorsey, Phys. Rev. B **46**, 8376 (1992).
[18] W.H. Press, S.A. Teukolsky, W.T. Vetterling, and B.P. Flannery, *Numerical Recipes in C* (Cambridge University Press, New York, 1992).
[19] L. G. Aslamazov and A. I. Larkin, Zh. Eksp. Teor. Fiz. Pis'ma Red. **9**, 150 (1968) [Sov. Phys. JETP **9**, 87 (1969)].

[20] If we allow ν to become negative, i.e., the string has a zigzag shape, one can show that $I(\mu,\nu)\to 0$ for $\mu\to 0$ and $-\nu\to 0$. Such a string, on the one hand, moves without dissipation, on the other hand, has an unbounded elastic energy.